Supporting Information

Molecular imaging of drug transit through the blood-brain barrier with MALDI mass spectrometry imaging

Xiaohui Liu[1], Jennifer L. Ide[1], Isaiah Norton[1], Mark A. Marchionni[2], Maritza C. Ebling[1], Lan Y. Wang[2], Erin Davis[2], Claire M. Sauvageot[2], Santosh Kesari[3], Katherine A. Kellersberger[4], Michael L. Easterling[4], Sandro Santagata[5], Darrin D. Stuart[6], John Alberta[2], Jeffrey N. Agar[7], Charles D. Stiles[2]*, and Nathalie Y.R. Agar[1,2,8]*

[1]Department of Neurosurgery, Brigham and Women's Hospital, Harvard Medical School, Boston MA

[2]Department of Cancer Biology, Dana-Farber Cancer Institute

[3]University of California San Diego, CA

[4]Bruker Daltonics, Billerica MA

[5]Department of Pathology, Brigham and Women's Hospital, Harvard Medical School, Boston MA

[6]Novartis Institutes for BioMedical Research, Emeryville, CA

[7]Brandeis University, Waltham MA

[8]Department of Radiology, Brigham and Women's Hospital, Harvard Medical School, Boston MA

* Correspondence should be addressed to N.Y.R.A. (Nathalie_Agar@dfci.harvard.edu) or C.D.S. (Charles_Stiles@dfci.harvard.edu).

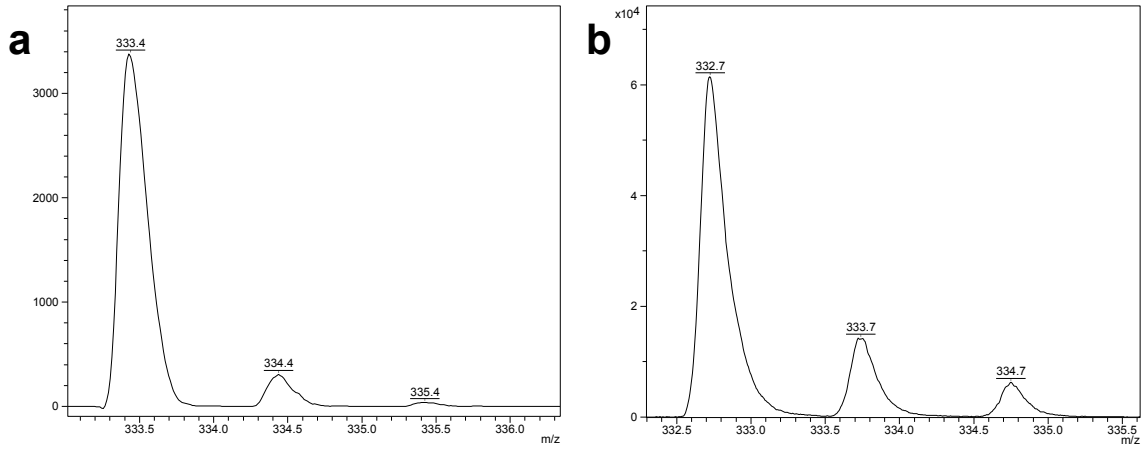

Figure S1 MALDI TOF spectra of (*A*) 5 µM of pure fluorescein and, (*B*) in mouse brain tissue at 10 µm thickness after a tail vein injection of 400 m/kg. The fluorescein signal (*m/z* 333.3±0.1) was used to image by MALDI MS**.**

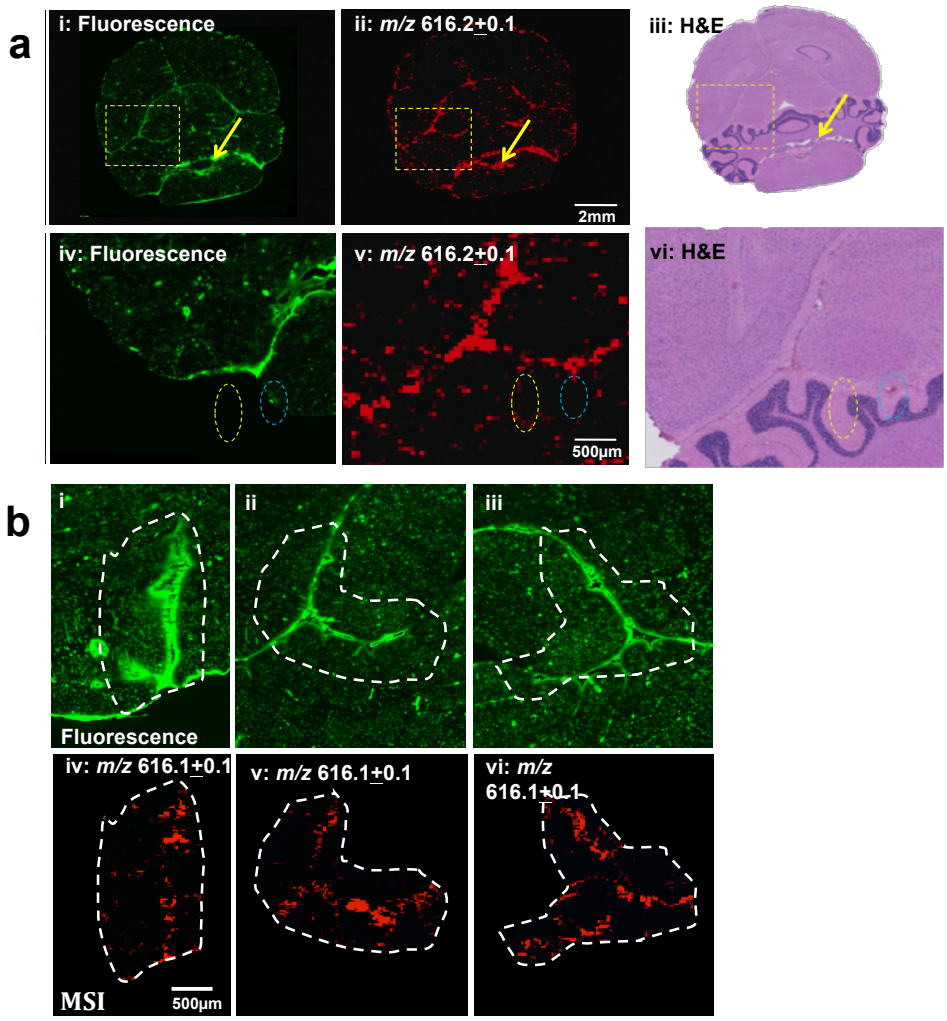

Figure S2 (*A*) Comparison of heme image (red, *m/z* 606.2±0.1) from MALDI MSI under 50 μm resolution with FITC image from fluorescence microscope (Ex-492 nm, Em-514 nm) on the same mouse brain section with pre-injected FITC and H&E staining of sister section. FITC was not detected by MALDI mass spectrometry. (*B*) Heme images (red, *m/z* 606.1±0.1) of selected regions in moue brain under 25 μm resolution and the comparison with fluorescence image from FITC (Ex-492 nm, Em-514 nm).

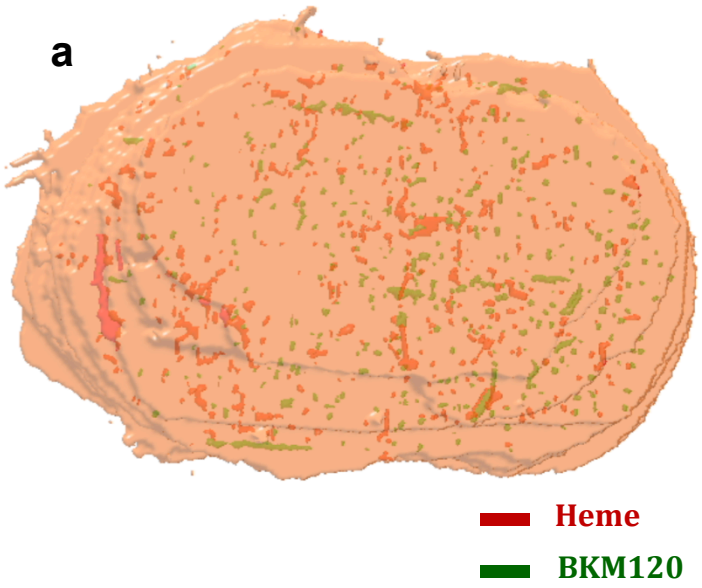

Video S1 3D reconstruction of BKM120 and heme distribution of coronal serial sections from a mouse brain after 4-hour dosing time and imaged by MALDI TOF. The sections were collected with 500 μm intervals and imaged at 100 μm spatial resolution. The 3D model was reconstructed using the software 3D Doctor after automated segmentation of individual MALDI images. The heme and BKM120 images obtained from the same section were displayed consecutively in the 3D model. Heme distribution is shown in red and BKM120 is displayed in green. BKM120 is not uniformly distributed across the entire mouse brain. High intensity drug signals are observed in the regions proximal to the lateral ventricles and cerebellum. Only sparse drug signal was observed in the frontal region.

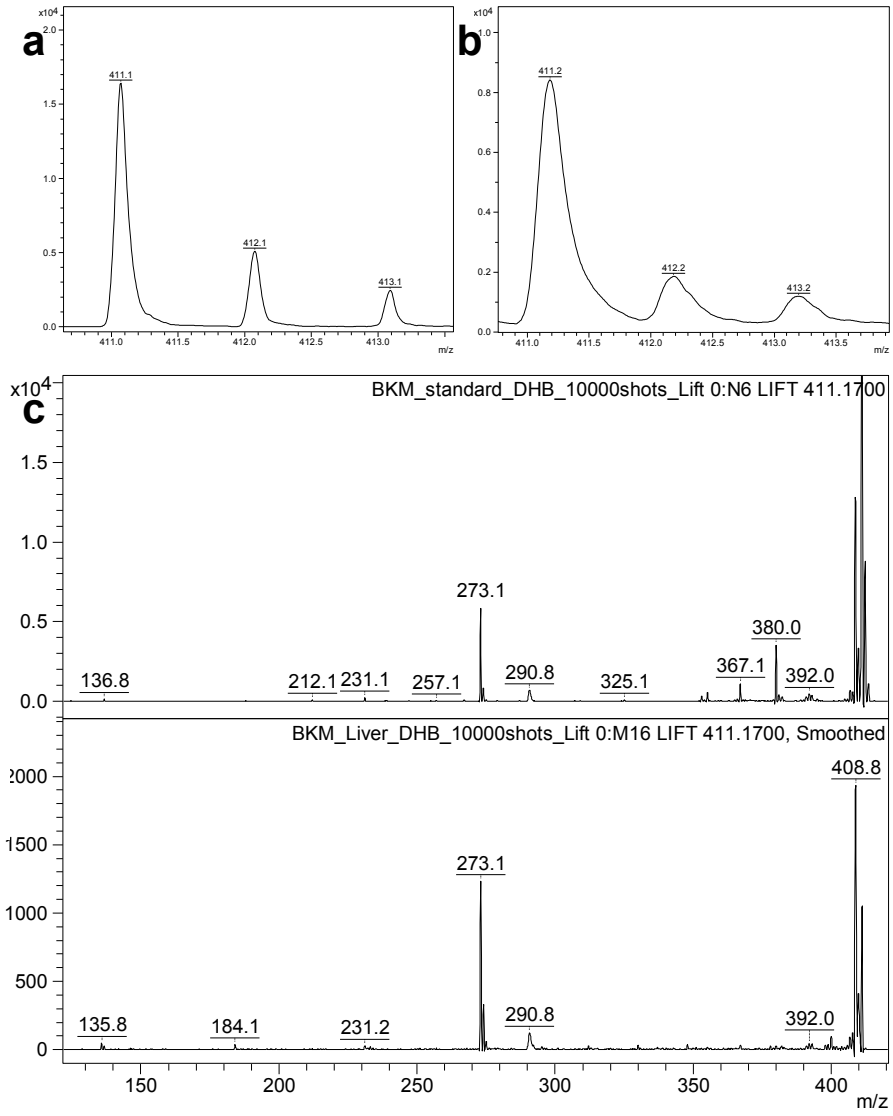

Figure S3 MALDI TOF detection of (*A*) pure BKM120 at 100uM concentration and, (*B*) detection of BKM120 in mouse liver at 4 hours after a single dose of 200 mg/kg. (*C*) MS/MS analysis of pure BKM120 (top) with observed fragments *m/z* 136.8, *m/z* 231.2, *m/z* 273.1, *m/z* 290.8, and *m/z* 392.0. MS/MS analysis of BKM120 from the dosed mouse liver tissue resulted in comparable fragments *m/z* 135.6, *m/z* 231.2, *m/z* 273.1, *m/z* 290.8, and *m/z* 392.0.

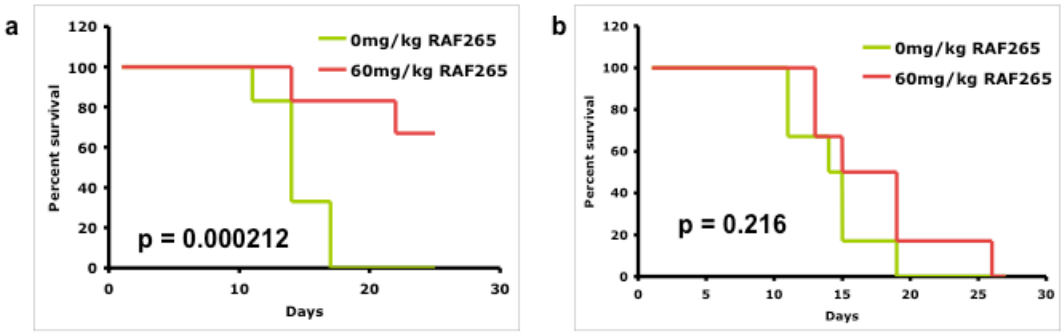

Figure S4 Subcutaneous versus intracranial implants treated with RAF265. The survival rate demonstrates the drug effect in (*A*) subcutaneous implants but little or no effect in (*B*) intracranial implants with 60mg/kg drug dosage.

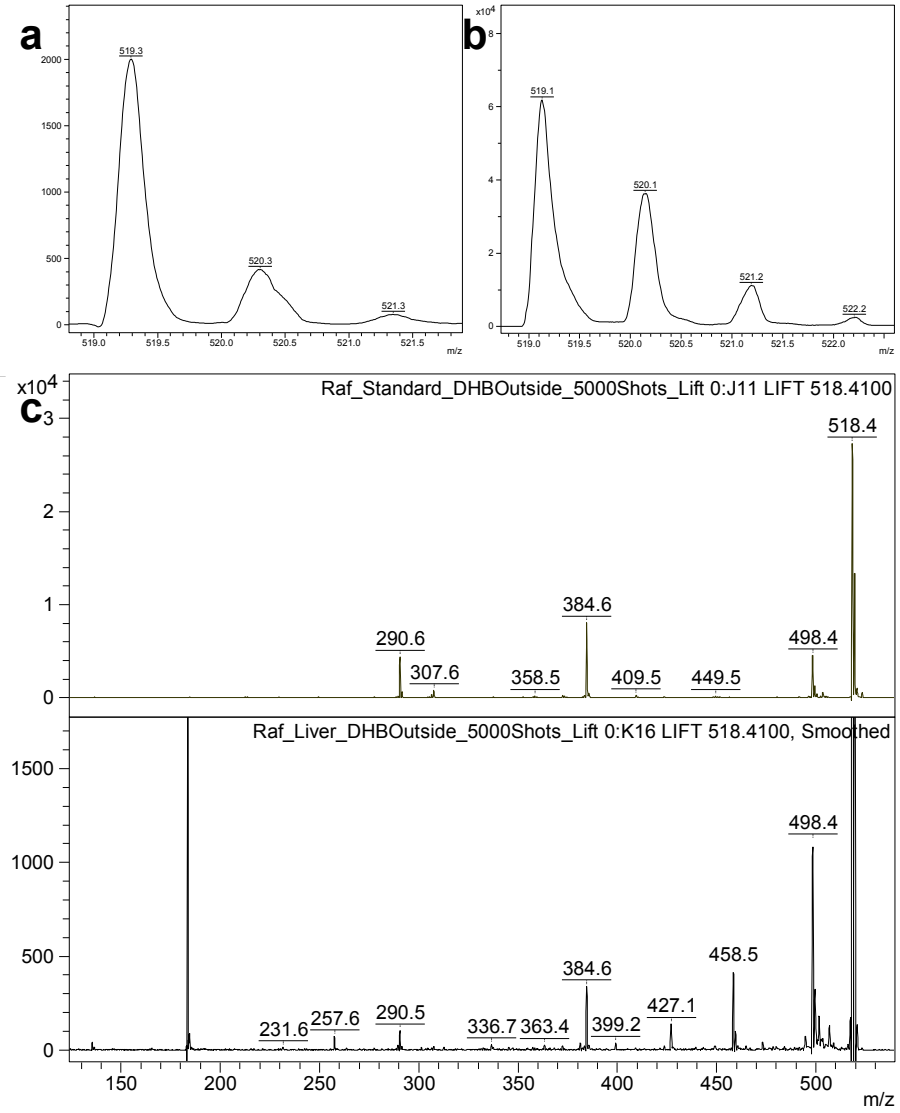

Figure S5 MALDI TOF analysis of (*A*) pure RAF265 at 50uM concentration, and (*B*) detection of RAF265 in mouse liver with a single dose of 60 mg/kg. (*C*) MS/MS analysis of pure RAF265 (top) with observed fragments at *m/z* 212.7, *m/z* 229.7, *m/z* 290.8, *m/z* 306.8, *m/z* 358.8, *m/z* 372.8, *m/z* 385.0, and *m/z* 498.9. MS/MS analysis of RAF265 from the dosed mouse liver tissue (bottom) resulted in comparable fragments *m/z* 290.5, *m/z* 384.6, and *m/z* 498.4.

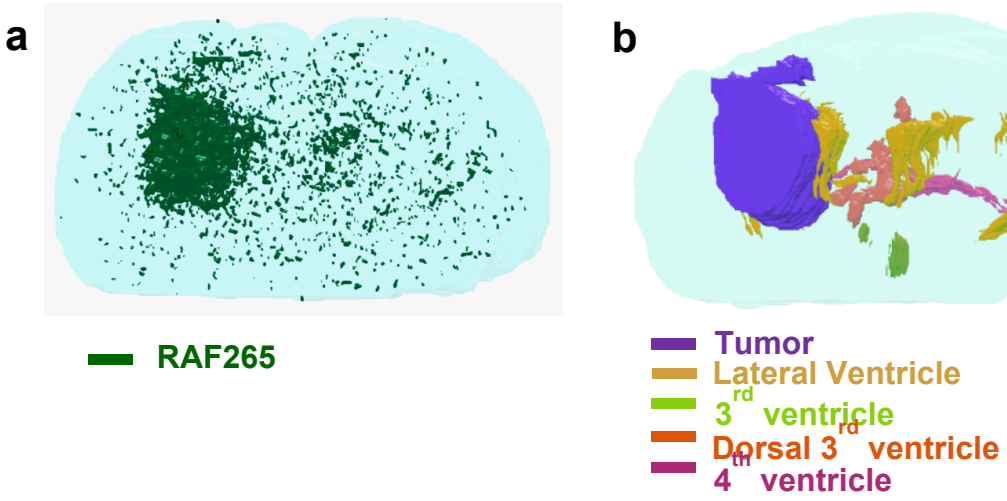

Video S2 3D reconstruction of (*A*) RAF265 (in green), (*B*) tumor (in purple) and ventricles (lateral ventricles in yellow, 3rd ventricle in light green, dorsal 3rd ventricle in orange, 4th ventricle in magenta) from optical images of H&E staining sections. Serial sections were collected with 30-50 μm intervals and imaged by mass spectrometer with 100 μm spatial resolution or microscope. 3D models were reconstructed using 3D Doctor.

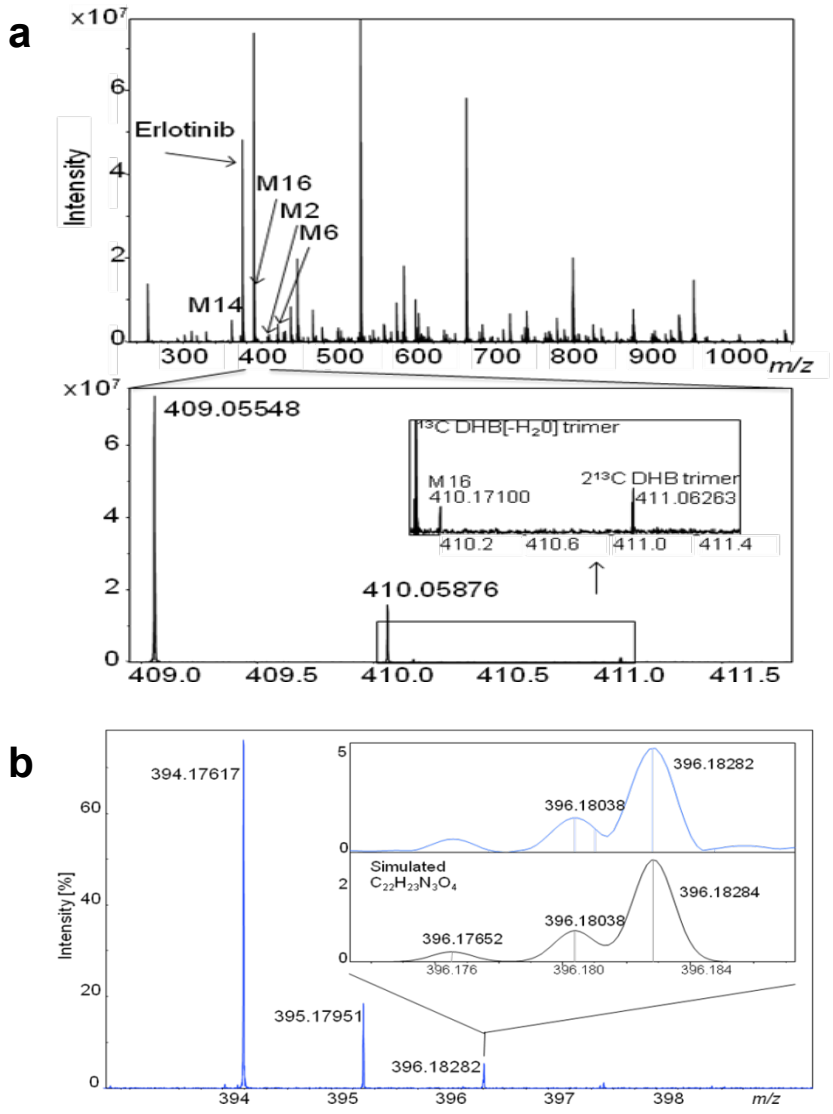

Figure S6 Detection of erlotinib and metabolites in mouse liver using MALDI FTICR. (**a**) Representative spectrum from mouse liver tissue with U87 xenograft tumor after 4hours' erlotinib treatment; below is the enlarged region for M16 ion. (**b**) Isotopic distribution of erlotinib (*m/z* 394.17617) with enlarged M+2 isotope indicating the isotopic fine structure from experiment (top) and simulation (bottom).

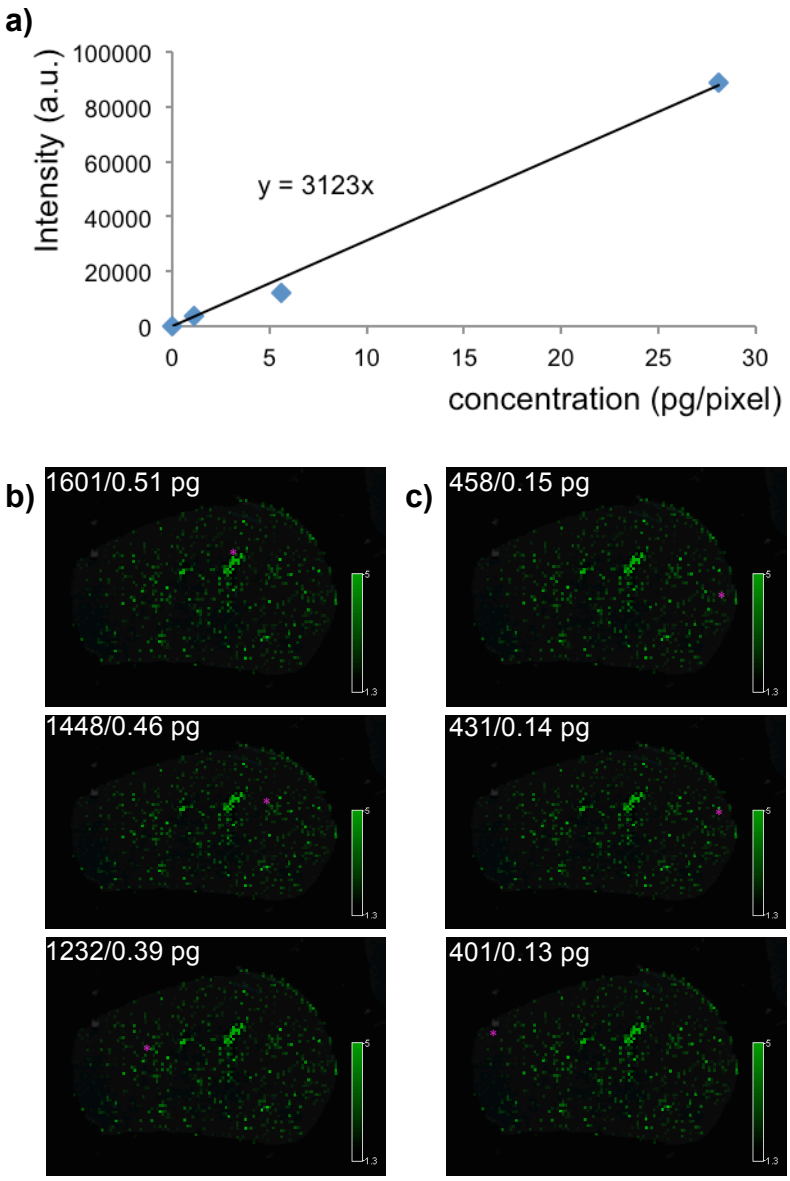

Figure S7. (**a**) A BKM120 serial dilution from the pure compound was spotted directly on a MALDI stainless steel target plate and analyzed. The x- axis corresponds to the concentration of BKM120 with the unit pg/pixel. Each pixel is 0.01mm^2, corresponding to the size of pixels from the MALDI images of BKM120 distribution. The y- axis corresponds to the peak intensity in the spectra. The plot was used to extract relative levels of BKM120 from distinct pixels. The (**b**) and (**c**) panels respectively highlight pixels of relative higher and lower intensity of BKM120. Selected representative pixels are juxtaposed by a pink star. The left number indicates the intensity in arbitrary units for the

selected pixel and the right number corresponds to the value transposed in picograms per pixel using the calibration curve presented in (**a**).